

# An uncertainty model for deep ocean single beam and multibeam echo sounder data

K. M. Marks and W. H. F. Smith

NOAA Laboratory for Satellite Altimetry, Silver Spring, MD, 20910, USA  
e-mail: [Karen.Marks@noaa.gov](mailto:Karen.Marks@noaa.gov)

Received: 11 June 2008/ Accepted: 7 December 2008

**Abstract** Comparing single beam and multibeam echo sounder data where surveys overlap we find that: 95% of multibeam measurements are repeatable to within 0.47% of depth; older single beam data can be at least as accurate as multibeam; single beam and multibeam profiles show excellent agreement at full-wavelengths longer than 4 km; archival sounding errors are not Gaussian; 95% of archival soundings in the northwest Atlantic are accurate to within 1.6% of depth; the 95<sup>th</sup> percentile error is about five times greater in pre-1969 data than in post-1968 data; many of the largest errors are located over large seafloor slopes, where small navigation errors can lead to large depth errors. Our uncertainty model has the form  $\sigma^2 = a^2 + (bz)^2 + (cs)^2$ , where  $2\sigma$  is approximately the 95<sup>th</sup> percentile error,  $z$  is the depth,  $s$  is the slope, and  $a$ ,  $b$ ,  $c$  are constants we determine separately for pre-1969 and post-1968 data.

**Keywords** Bathymetry, Error, Uncertainty, Micronesia, Atlantic, Statistics

## Introduction

The vast majority of the ocean lies beyond the boundaries of national territorial claims and mapping responsibilities, and is not subject to the stringent standards applied to areas surveyed for the purpose of safe navigation. In this area, which we will call the “deep ocean,” data available to the public at no cost comprise a heterogeneous mix of new and old navigation and echo sounder technologies deployed along essentially random track lines covering only a few percent of the ocean basins. In some areas the majority of the data were collected with the oldest and least accurate means, due to a decline in the funding of curiosity-driven exploration since the early 1970s (Smith, 1993, 1998). Mapping the deep ocean basins requires bringing multibeam and single beam echo sounder data, the latter including older, poorly navigated data, into a coherent synthesis, with some intelligent gap-filling scheme.

Smith and Sandwell (1994, 1997) have demonstrated the value of using sea surface gravity anomalies derived from satellite altimetry to guide the interpolation of gaps between ship surveys in the deep ocean basins. Their method has been adopted in the United States by a tri-agency task force of the National Oceanic and Atmospheric Administration, the Naval Oceanographic Office, and the National Geospatial-Intelligence Agency, and internationally by GEBCO, the committee for the General Bathymetric Charts of the Oceans. To date, however, their method gives equal weight to all echo sounder data, and makes no attempt to

account for varying uncertainties or to build an error model for the solution. In order to extend their process to include error-weighted data assimilation and solution uncertainty modeling, some idea of the uncertainties in the input data will be required.

In this paper, our aim is to develop an uncertainty model that can be applied to single beam and multibeam echo sounder data, both new and old, to facilitate deep ocean mapping by synthesis of archival data. For this purpose, we must characterize the disagreements among heterogeneous measurements, which may be much larger than the theoretically expected uncertainties derived from engineering analyses of measurement systems. In recent years, some very high quality deep-ocean multibeam echo sounder data have been made readily available, allowing us to analyze the repeatability of multibeam surveys and to compare multibeam soundings to archival single beam soundings.

We examine data in two geologically distinct environments facilitating two kinds of analyses. In the western Pacific Ocean where atolls rise from about 4.5 km depth, there are evidently well-navigated single beam survey tracks that were later repeated two or three times by multibeam surveys, in one case for about 800 km of track line. This allows us to assess the repeatability of measurements and to characterize the spatial resolution and accuracy of single beam versus multibeam echo sounder data. In the northwest Atlantic Ocean, a broad area of continental slope with nearly 5.5 km of relief is covered by a recent multibeam survey, and we compare archival survey line data crossing this area to the new

multibeam grid. This allows us to develop a model for expected bathymetric uncertainty.

#### Previous Studies

Smith (1993) identified systematic bias errors in archival deep ocean survey data digitized from single beam analog records by examining the discrepancy in depths at points where two survey lines crossed. His analysis primarily served to identify gross blunders in the digitizing of analog records and in the conversion of acoustic travel time to depth. He concluded that uncertainties smaller than 2.5% of depth would be difficult to detect by his method. Our study may be viewed as an extension of Smith's, making use of the vast amount of new multibeam data that has become available: while Smith could only study depth discrepancies at single beam survey track intersections, we can compare single beam echo soundings to multibeam soundings in areas of 100% multibeam coverage.

Other studies include Hare (1995), who presented an error budget for modern multibeam swath mapping systems derived from theoretical considerations of the instrument's engineering. His error budget does not include the discrepancies between heterogeneous measurement systems that one must address in deep ocean synthesis mapping. Jakobsson et al. (2002) assigned uncertainties to heterogeneous data sources and then used Monte Carlo simulations to estimate how errors along survey lines would propagate into errors in derived bathymetric grids. Their study does not appear to have derived the uncertainties empirically, as we do here. Calder (2006) compared archival data to modern multibeam surveys, but both were in the shallow water hydrographic context. Finally, the International Hydrographic Organization sets forth internationally agreed goals for bathymetric survey uncertainty in the context of charting hazards to surface vessel navigation by modern means (IHO, 2008). The IHO standard is one which future shallow water surveys should meet, and is not meant to characterize uncertainty in data collected previously.

#### Study Area 1 - Micronesia

It is hard to find single beam and multibeam tracks that overlap because the vast oceans are only sparsely covered by ships. But in a region west of the Caroline Islands of Micronesia, ships proceeding between Guam and New Guinea have sometimes taken the same route, perhaps because there are only a few north-south passages between the atolls (Figure 1). Here we find well-navigated single beam depth survey track lines that

were subsequently covered by two or three different multibeam swaths (Figure 2).

#### Data

We obtained the single beam echo sounder data in this area from the National Geophysical Data Center GEODAS database (NGDC, 2003; <http://www.ngdc.noaa.gov/mgg/geodas/trackline.html>).

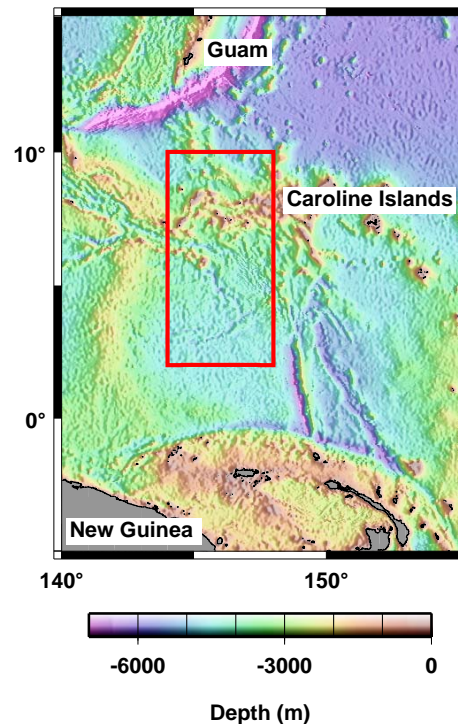


**Fig. 1** Color shaded-relief image of satellite bathymetry (Smith and Sandwell, 1997) in the western Pacific Ocean. Micronesia study area is outlined by red box, and includes deep water to the south and a region of atolls and seamounts west of the Caroline Islands

The data were collected in 1992 by R/V *Moana Wave* utilizing GPS navigation and a 3.5 kHz, 30 degree beam echo sounder system recorded on an analog strip chart with a 1-s sweep and subsequently digitized every 5 to 15 minutes (roughly 1.5 to 4.5 km along-track), or more frequently where depth changed rapidly. We also used single beam echo sounder data from R/Vs *Vema* and *Mahi*, which were collected in 1977 and 1970, respectively. Both were navigated using Transit satellite with dead-reckoning between fixes. *Vema* had a 3.5 kHz 60 degree echo sounder. The instrument is unspecified in the *Mahi* metadata. Carter (1980) sound velocity corrections were applied to all these single beam echo sounder data.

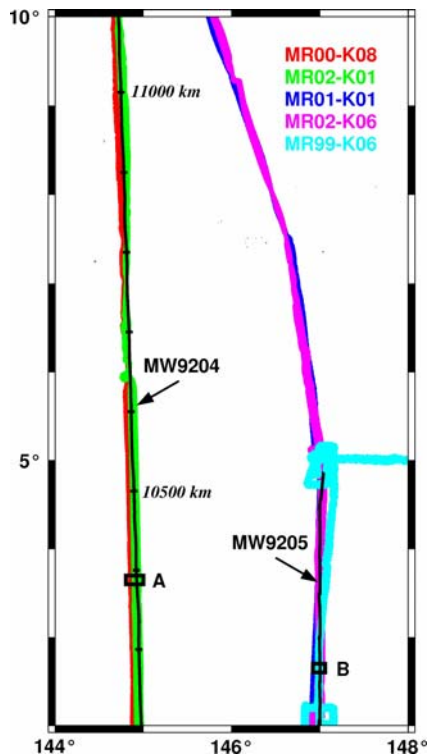


**Fig. 2** Overlap of multibeam swaths (*color*) and single beam surveys (*black lines*) in the Micronesia study area (outlined in Fig. 1)

We obtained the multibeam echo sounder data as *xyz* ping files from the web site of the Japan Agency for Marine-Earth Science and Technology (JAMSTEC; <http://www.jamstec.go.jp/mirai/>). The swaths were collected between 1999 and 2002 by R/V *Mirai*, using a Sena Advanced Integrated Navigation System (version 19) and a Seabeam 2112.004 multibeam system. The data were processed, cleaned, and quality controlled by JAMSTEC using HIPS/SIPS 5.3 (CARIS) software. Processing included rejecting side beams (beam numbers 1-12 and 131-151), rejecting spike noise data, deleting location error data, and converting to *xyz* (ascii) format.

Figure 2 shows that multibeam swaths MR00-K08 and MR02-K01 overlap each other and also traverse the MW9204 single beam track. Likewise, multibeam swaths MR01-K01, MR02-K06, and MR99-K06 overlap each other and traverse the MW9205 single beam track.

#### Repeatability of Multibeam Echo Sounder Depths

Many tens of millions of individual depth measurements are collected during a typical multibeam survey, providing dense coverage along a swath. As an illustration, we consider the data in box A in Figure 2. Within this box alone are over 12,000 *xyz* data points from survey MR00-K08, and over 15,000 points from MR02-K01, in the files made available through the

JAMSTEC web site. Far fewer data are collected by single beam surveys. Along track MW9204 there are 24 depth measurements within this box. However, the spacing of single beam echo sounder data is controlled by the sampling frequency with which the analog records are digitized.

To facilitate comparison of the overlap areas in the multibeam swaths, we produced a grid of each swath from the individual *xyz* points in the available files. We used the GMT (Wessel and Smith, 1998; <http://gmt.soest.hawaii.edu>) routine “surface,” an adjustable tension continuous curvature surface gridding algorithm, to form a grid at 6 arc-second spacing in latitude and longitude (roughly 200 m), and then used “blockmean” and “xyz2grd” to create a mask that was applied to the grid so that it holds values only in cells that contained one or more of the original *xyz* points. In what follows, GMT routine “grdtrack” was used whenever we interpolated a grid to given *xy* points.

We assessed the fidelity of each multibeam grid to the original *xyz* data by interpolating the grid at the locations of the original *xyz* points and examining the difference between the original and interpolated *z* values. A histogram of these differences for MR00-K08 is shown in Figure 3a. The standard deviation is 5.7 m, and 95% of the differences are less than 11.2 m. The typical depth along the swath is -4137 m, for comparison; thus, gridding and interpolation introduces an error around 0.14%.

To compare depths from overlapping multibeam swaths we calculated the differences between *xyz* points from swath MR00-K08 and the overlapping MR02-K01 multibeam grid. The results are plotted in a histogram in Figure 3b (black lines). For these overlapping multibeam swaths the standard deviation of the differences is 10.9 m, 95% of the differences are less than 19.3 m, or around 0.47% of the depth. Note that here we compare point values to an interpolated grid, rather than gridded values to gridded values, so that the ~0.14% gridding and interpolation error enters only once, not twice.

For purposes of viewing these differences in map form (Figure 4a), we subtracted multibeam grid MR02-K01 from MR00-K08. Differences are positive in the east and negative in the west, indicating a systematic tilt of one survey relative to the other, suggesting that there may be a roll bias error in one or both swaths. Roll bias is a misalignment of the vertical reference supplied to the swath mapping system; it should produce errors that are greatest in the outer beams and also increase with depth. The swath overlap here is about 6.6 km wide and the differences span about 15 m, for a tilt of about 2.2 m/km, or a roll bias error of about 2 milliradians.

The crosses and circles cutting across the difference grid in Figure 4a mark the *xy* positions of one “fan” of values from one ping of each of the surveys

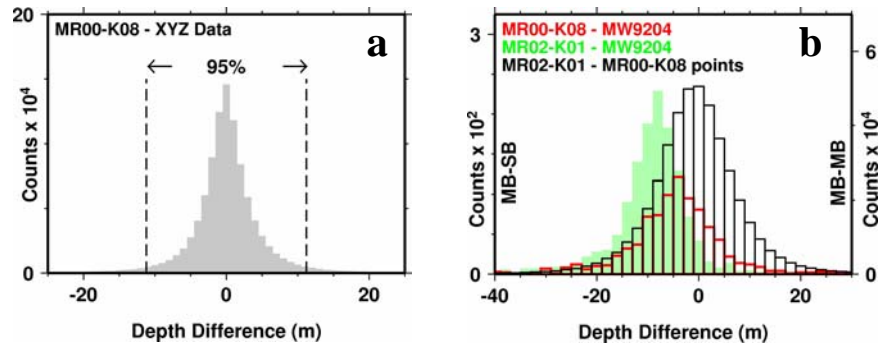


**Fig. 3** (a) Histogram of differences between original *xyz* data values and values interpolated from corresponding MR00-K08 multibeam grid. 95% of differences are less than 11.2 m, or 0.14%. (b) Histograms of depth differences obtained by subtracting single beam (MW9204) depths from multibeam (MR00-K08 is red; MR02-K01 is green) depth grids, and from subtracting MR00-K08 *xyz* data points from the overlapping

MR02-K01 multibeam grid (black). The width of the histogram of differences between *xyz* points and the overlapping multibeam grid (black) is wider than the histograms of differences between single beam and multibeam (red and green), showing that single beam echo sounder measurements may be at least as accurate as those of multibeam echo sounder systems

MR00-K08 and MR02-K01, respectively. The ping depths from each fan are plotted against longitude in Figure 4b. In Figure 4b, the red (and green) lines are from the gridded swath data, and the red (and green) dots are the *xyz* data directly from the ping files. This shows how well the grids honor the raw *xyz* points profiled here. The white star is a single beam echo sounding from MW9204 (also located as a white star on Fig. 4a); its depth agrees well with the multibeam echo sounder depths. The center portions of the overlapping swaths have similar depths while the depth differences between MR00-K08 and MR02-K01 increase towards the outer beams of the profiles. This is consistent with a roll bias error.

#### Single Beam versus Multibeam Echo Sounder Data

We interpolated the MR00-K08 and MR02-K01 multibeam grids to the sample points of the MW9204 single beam echo soundings, and then subtracted the single beam depths from the interpolated multibeam depths. These differences are plotted as histograms in Figure 3b. The histogram shows there is a -9 m median offset for the MR02-K01 and MW9204 depth differences (green area), and only a -4 m median offset for the MR00-K08 and MW9204 depth differences (red lines). An interesting result is that the histogram of differences between gridded multibeam depths from MR02-K01 and *xyz* points from MR00-K08 (black lines) appears wider than the red and green histograms of differences between multibeam and single beam depths. In other words, the variance of the differences of two multibeam values is larger than the variance of the differences of a multibeam value with a single beam value. Thus, single beam echo sounder measurements may be at least as accurate as multibeam echo sounder measurements. The multibeam

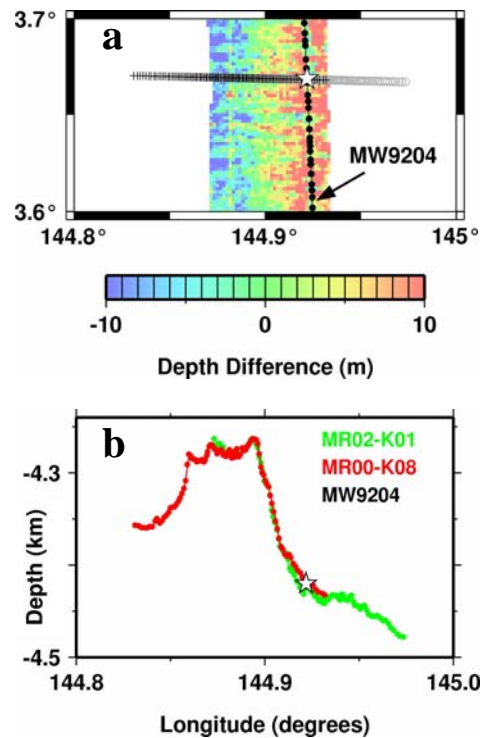


**Fig. 4** (a) Depth differences obtained by subtracting multibeam grid MR02-K01 from MR00-K08 in box A (see Fig. 2). An east-west tilt possibly caused by roll bias is indicated by positive (orange) values grading to negative (blue). Overlapping ping fans from MR00-K08 (crosses) and MR02-K01 (gray circles) are profiled in (b); single beam MW9204 samples are black dots and the sample shown as a white star is also in (b). (b) Profiles of overlapping ping fans from MR02-K01 (green) and MR00-K08 (red); differences in the outer beams are consistent with roll bias. Multibeam gridded depths (lines) match their point depths (dots). The single beam depth (white star) matches those from multibeam

depths combine both nadir and off-nadir narrow beams, and the latter will be more uncertain because of refraction errors, motion artifacts, and other factors. The single (wide) beam measurement samples a wider patch of the ocean floor than the nadir beam of the multibeam system, so the single beam uncertainty includes the variance of the ocean floor within the sampled patch (next section).

### Sampling of the Seafloor by Single Beam Echo Sounders

Next we examine the patch of seafloor that is ensonified by an ideal single beam echo sounder acoustic pulse. The sampled volume is shaped like a cone with its axis directed downwards. The area of seafloor ensonified by the pulse is approximately circular in shape and its size depends on the transducer beam width, the pulse width, and also on the depth of the seafloor. Because the pulse traveling the shortest distance is reflected back from the seabed first, it is commonly assumed that single-beam sounders measure the shallowest point within the ensonified patch.

In Figure 5a we show depths from a portion of multibeam swath MR02-K01. Single beam survey MW9204 tracks north-south along this swath. For this example we have chosen one single beam echo sounding measurement (white star) to focus on, and have highlighted the patch of seafloor beneath it that would be ensonified by the acoustic pulse, assuming a vertical transducer and ignoring pitch and roll. We calculated the diameter of the patch based on a 30 degree beam width and an average depth of 4160 meters (radius = depth \* tan(15°)). Each xyz point from the MR02-K01 multibeam survey lying within the circular-shaped patch is plotted as a black dot.

We plot these multibeam values within the ensonified patch in a 3-D bar graph in Figure 5b. The red dot is the shallowest ping depth, the blue dot is the deepest ping depth, and the white star is the depth from the one single beam echo sounding measurement we focus on here. It appears that the single beam pulse in fact measures the average depth in the ensonified patch, rather than the shallowest depth, as is generally assumed. A histogram of the pings in this patch (Figure 5c) shows that the single beam depth of -4156 m is very close to the computed mean of -4153 m. The sonar receiver gathers returns from all the reflections that have undergone constructive interference from within the ensonified patch, and this reflected energy peaks about the mode of the depth distribution within the patch. When the analog graph of returned energy is digitized the digitizer must choose some point (maximum, first discernible arrival, or other) to identify the measured return. In this example, it appears that the measured depth is closer to the average depth, and not the shallowest depth.

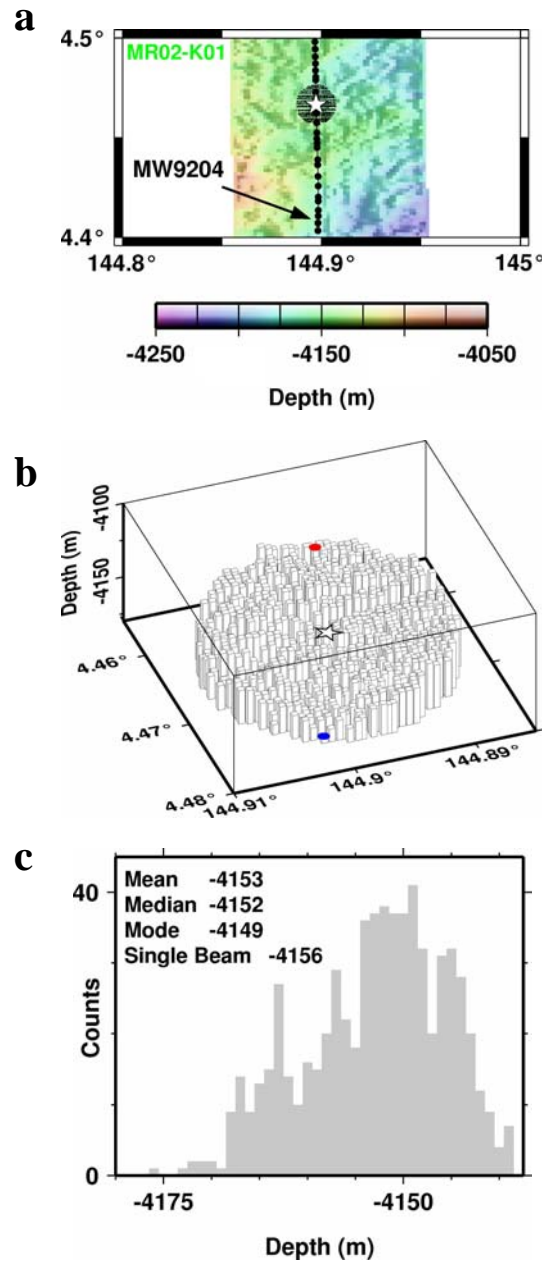


**Fig. 5(a)** A single beam echo sounder sample (*white star*) and the patch of seafloor below it that would be ensonified by its 30 degree wide echo sounder during an acoustic pulse, assuming no pitch or roll. Each xyz point from the MR02-K01 multibeam survey lying within the patch is plotted as a *black dot*. Large *black dots* are MW9204 single beam samples. The gridded MR02-K01 depths are imaged in color shaded-relief. **(b)** 3-D bar graph of the multibeam pings within the ensonified patch in (a). The shallowest ping depth (*red dot*), deepest ping depth (*blue dot*), and the single beam depth (*white star*) are plotted. The single beam depth nearly fits the average depth within the ensonified patch, and not the shallowest depth, as is commonly assumed. **(c)** Histogram of xyz points in patch shown in (a). The single beam depth of -4156 m is approximately equal to the mean depth of the patch

To test whether this result holds for the entire MW9204 (and MW9205) survey, we developed a program that calculated, at each single beam echo sounder sample location, the shallowest, the deepest, and the mean multibeam depths within the corresponding ensonified patch, as well as other statistics. The result is that single beam depths are systematically deeper than the shallowest multibeam depth within the corresponding patches. We find that the single beam echo sounder system does a rather good job of averaging the depths within the patch it samples.

#### Spatial Resolution of Single Beam and Multibeam Echo Sounder Systems

We made a cross-spectral coherency-squared analysis between pairs of depth sequences from the MW9204, MR02-K01 and MR00-K08 data along profiles between 3.3° and 5.8° north latitude (see Figure 2), where the depths are mostly in the range -4000 to -4500 meters and show abyssal hill fabric. Coherency-squared measures the square of the linear correlation coefficient between the two data types in the pair, as a function of spatial wavelength along the profile; data analysis was via the GMT tool “spectrum1d.” A squared coherency of 1 means perfect correlation between the two inputs, while a value of 0.5 can be interpreted as a signal-to-noise ratio of 1:1 in one input if the other input can be assumed to be noise-free. The resolved spatial scales in the data are about half the full-wavelengths where the coherency is greater than 0.5, and are well-resolved when the coherency is much greater than 0.5.

We performed the analysis two ways: 1) between north-south profiles at overlap points extracted from the two multibeam grids, and 2) by comparing the MR00-K08 grid sampled at the MW9204 points against the MW9204 data (see Figure 6). In both cases, the coherency-squared is essentially 1 for full-wavelengths longer than about 7 km. At shorter scales, coherency-squared decreases. For analysis 1 (crosses in Figure 6) the two multibeam systems at full grid resolution (200 m sampling) show high coherency to around 2.5 km full-wavelength. For analysis 2 (gray dots in Figure 6), the coherency-squared begins to depart substantially from 1 at around 4 km full-wavelength, that is, at half-wavelength scales comparable to the diameter of the single beam footprint. We find that the single beam system is measuring the seafloor as faithfully as the multibeam system at the spatial scales that can be resolved by the diameter of the beam footprint and the sampling rate with which the analog recordings are digitized.

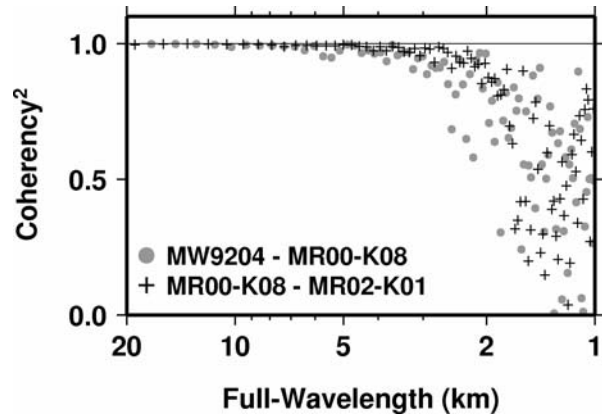


**Fig. 6** Cross-spectral coherency analysis between MW9204 and MR00-K08 (gray dots) and MR00-K08 and MR02-K01 (crosses). Perfect correlation has a coherency<sup>2</sup> of 1, and no correlation is 0. The multibeam systems are coherent to about 2.5 km full-wavelength, and the single beam to about 4 km full-wavelength. Single beam and multibeam resolve the same features at scales greater than about 2 km- the approximate width of the patch ensonified by a single beam echo sounder acoustic pulse

#### Using Single Beam to Find Errors in Multibeam Echo Sounder Data

We examine the differences (Figure 7a) between swaths MR02-K06 and MR99-K06 in box B (outlined in Figure 2). This difference grid, which was created by subtracting the MR99-K06 multibeam grid from the MR02-K06 one, displays a strong east-west tilt, as is evidenced by negative values grading to positive. As before, this is consistent with a roll bias error in one or both multibeam swaths.

There are two single beam tracks in the NGDC archive, V3403 and 70042204, that cut across the difference grid. Multibeam depths from swaths MR99-K06 and MR02-K06 are plotted along track V3404 in Figure 7b, and along track 70042204 in Figure 7c. In Figure 7b, the multibeam depths from MR02-K06 (purple line) match the V3404 single beam depths (black dots), and in Figure 7c the MR02-K06 depths (purple line) match the 70042204 single beam depths (black dots). In both figures the multibeam depths from MR99-K06 (blue lines) are tilted with respect to the single beam depths. It appears multibeam swath MR99-K06 contains the roll bias error, which shows up in both the difference grid (Figure 7a) and as tilts in Figures 7b and 7c. Also, it is interesting to note that both multibeam swaths are from the R/V *Mirai*'s Seabeam 2112.004 system operating in ~4450 m of water, yet the system seems to have operated in two different modes on these two cruises, as the swath widths are different.

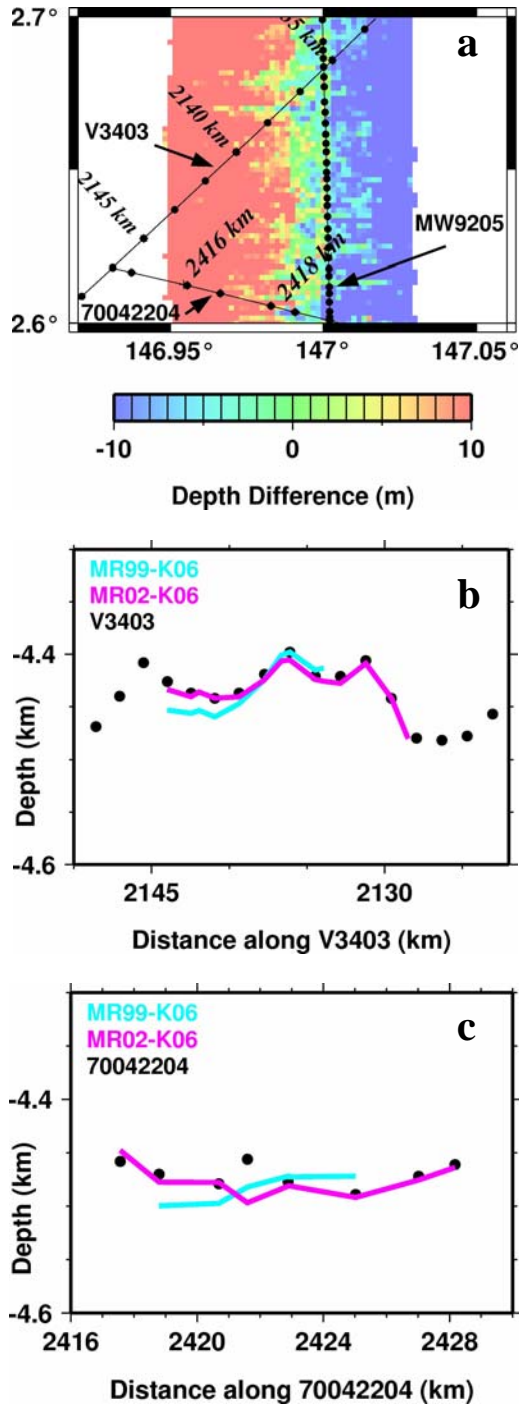


**Fig. 7** (a) Depth differences obtained by subtracting multibeam grid MR99-K06 from MR02-K06 in *box B* (see Fig. 2). As described in Fig. 4 caption, there is an east-west tilt of the difference grid. Single beam surveys V3403 and 70042204 are plotted in (b) and (c). Depths from MR02-K06 multibeam grid (purple lines) match V3403 (b) and 70042204 (c) single beam measurements (black dots), but depths from MR99-K06 multibeam grid (blue lines) appear tilted, which may be evidence of roll bias

### Study Area 2 – Northwest Atlantic Continental Slope

Here we compare 171,078 point soundings along 192 track lines archived at NGDC with a multibeam grid (that we abbreviate as the CCOM grid) available from the University of New Hampshire Center for Coastal and Ocean Mapping/Joint Hydrographic Center (<http://ccom.unh.edu>). The NGDC data are from the same GEODAS data base cited above and were collected with a variety of sounding and navigation technologies between 1955 and 2004. The GEODAS MGD77 format includes not only single beam surveys but also multibeam surveys, where the latter have placed center beam data into the GEODAS cruise format. The CCOM multibeam grid is on a spacing of 0.001 degrees and was produced from surveys made in 2004 and 2005.

Our comparison is made by interpolating the CCOM grid to the NGDC archive sounding points, and we examine only points at which this interpolation could be made by GMT program “grdtrack” using a bilinear interpolant. The number of point soundings that we studied from each cruise is thus a function of the overlap of that cruise with the CCOM grid. The data locations are shown in Figure 8.

The cumulative number of soundings and number of cruises from the NGDC archive are shown in Figure 9. Thirty percent of the cruise files, containing 15% of the total soundings, were collected before mid-1967, when Transit satellite navigation was made available. Ninety-five percent of the cruises, containing 85% of the soundings, were collected prior to the completion of the GPS navigation system in 1994. The number of cruises shows its most rapid increase in the early 1970s, consistent with the findings of earlier studies that suggested that deep water geophysical cruise activity peaked in the early 1970s (Smith, 1993). The number of soundings increases most rapidly in the late 1980s, as multibeam systems come into use.

For each point sounding we can compare the depth in the NGDC archival cruise file,  $d_i$ , with the depth in the CCOM grid,  $g_i$ ; the difference  $e_i = d_i - g_i$  we will call an “error.” However, we recognize that this “error” combines the errors in both the archival soundings and the CCOM grid, plus whatever additional error may be made in interpolating the grid to the sounding point. For data collected with navigation predating the WGS-84 position standard, there may also be an error component due to horizontal displacement of the point sounding. Metadata on the point values are insufficient to permit us to correct for this, and we deal with it below by considering an error component proportional to seafloor slope. A posteriori justification for ignoring horizontal datum shifts between ellipsoids comes from the result that navigation errors we find in old data are much larger than changes in horizontal datums.

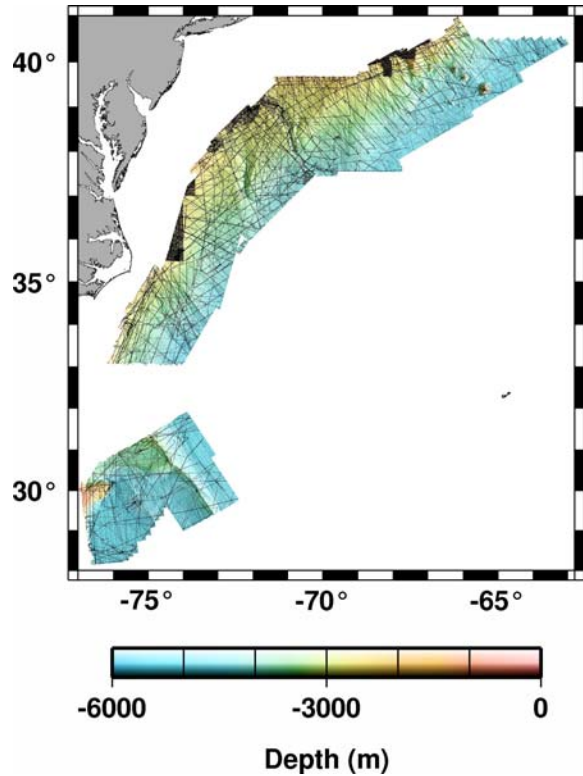


**Fig. 8** Color shaded-relief image of CCOM multibeam bathymetry over the northwest Atlantic continental slope study area. Dots are point soundings archived at NGDC

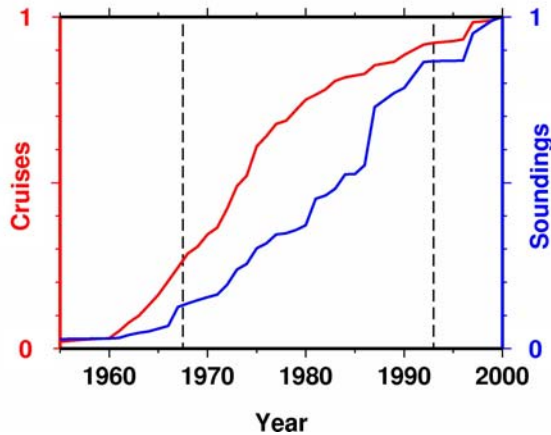


**Fig. 9** Cumulative number of cruises (red line) and soundings (blue line) spanning 1955 through 2000. There was a rapid increase in the number of cruises when oceanic research peaked in the early 1970s, and the advent of multibeam systems increased the number of soundings in the late 1980s

The International Hydrographic Organization proposes, in its standard “S-44,” that the 95% confidence point for the total vertical uncertainty in a sounding

equation should be a value,  $\epsilon_{95}$ . The value is determined by an

$$\epsilon_{95} = \sqrt{a^2 + (bz)^2} ,$$

in which  $z$  is the true depth and  $a$  and  $b$  are constants set by the “order” of the survey, essentially a classification indicating how critical is the need for accurate bathymetry. This standard is meant to apply to future shallow water hydrographic surveys, and is not meant to characterize typical uncertainties in archival deep water data. Nevertheless, we feel that the functional form of the error as given above is a useful one for our study, as it is the form expected when the error combines uncorrelated errors in travel time and sound velocity. Unless otherwise stated, we will use the 5<sup>th</sup> edition of S-44 (IHO, 2008) “Order 2” values, which are the least stringent and are meant to apply to surveys in water deeper than 100 m where it may be presumed likely that no hazards to navigation exist. According to this standard,  $a = 1$  meter and  $b = 2.3\%$  of depth.

We determined the empirical 95<sup>th</sup> percentile point of the cumulative distribution of our  $|e_i|$  data, grouped in 13-year bins (Figure 10); these 95<sup>th</sup> percentile points correspond closely to the IHO S-44 standard ( $\epsilon_{95}$ ) after 1968, but are about 5 times worse before that. Here we interpret the standard as if it applied to these differences, assuming the CCOM grid depth to be “true.” A detail map (Figure 11) shows that points where  $|e_i| > \epsilon_{95}$  are often located in areas of large topographic slope, such as at the shelf edge and in submarine canyons.

To examine the importance of navigation errors and slope, we computed a seafloor slope magnitude grid,  $s$ , by first smoothing the CCOM grid and then taking finite differences. Smoothing was by GMT routine “grdfilter,” employing a convolution with a 5 km diameter cosine bell filter; this has a full-wavelength at half-amplitude of 5 km, and removes full-wavelengths shorter than 2.5 km. The resulting smoothed magnitude grid resolves the signal of canyons in the sea floor. We operated on a smoothed grid over this distance for two reasons. First, the slope within the ensonified patch is probably not a major source of error, because the average depth is what is measured (Figure 5b). Second, the depth error due to a navigational error may be expected to have a magnitude roughly proportional to the mean slope over a distance typical of navigation errors. For modern GPS navigation this is much less than the width of a beam sample patch in deep water, but for older cruises it can be much larger.

We extended the S-44 error formulation by considering a model in which the variance of the errors has the form

$$\sigma^2 = a^2 + (bz)^2 + (cs)^2,$$

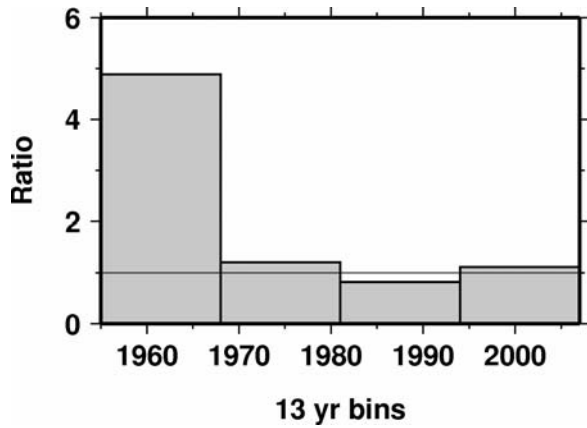


**Fig. 10** Ratio of observed errors to the IHO S-44 standard (see text). After 1968, the observed errors nearly meet the IHO standard. Prior, they were about five times as large

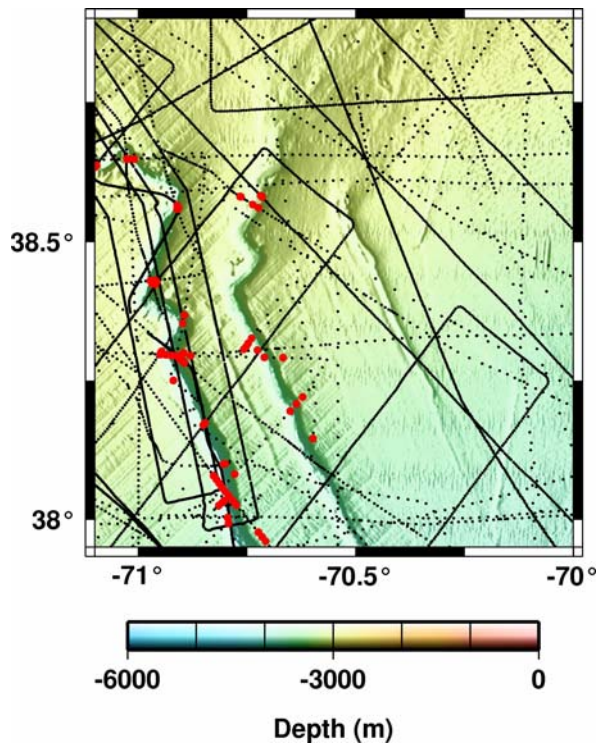


**Fig. 11** NGDC point soundings (*black dots*) plotted on seafloor depth from the CCOTM multibeam grid, in color shaded-relief, illuminated from the east. Soundings that exceed the IHO S-44 standard (*red dots*) correlate with sharply sloping topography

with  $z$  the depth and  $s$  the smoothed slope. We tried determining constants  $a, b, c$  that would best characterize the error distributions we found. The 5<sup>th</sup> edition of S-44 explicitly states that the uncertainties shall be assumed to have a Gaussian distribution. We found that our  $e_i$  values have a distribution that is decidedly not Gaussian; although the vast majority of them (sometimes nearly 95% of them) may be close to Gaussian. However, the

last few percent of the distribution always exhibit values much larger than would be found in a truly Gaussian distribution, or even a two-sided exponential (“Laplace”) distribution. In other words, a few large errors always occur; the data inevitably have “outliers.” We found that many of the larger outliers result from data collection blunders.

We used quantile-quantile plots to characterize the error magnitudes and assess the departure from Gaussian statistics. To do this for a set of  $e_i$  values, we sort the values into non-decreasing order, then if the values are numbered from 1 to  $N$  the  $i$ -th value is assigned a quantile,  $q_i$ , such that

$$\frac{i-0.5}{N} = \frac{2}{\sqrt{2\pi}} \int_{-\infty}^{q_i} \exp(-t^2/2) dt.$$

This procedure assumes that the median of the data is expected to be zero; that is, that the depth differences do not show a systematic bias.

We tried fitting values of  $a, b, c$  as above to determine a  $\sigma$  such so as to minimize

$$E^2 = \sum_{|q_i| \leq 1.96} \left( q_i - \frac{e_i}{\sigma} \right)^2,$$

the total squared error of departure from a one-to-one line, taking the sum over the middle 95% of the data. Initially we tried fitting such error models to each cruise individually, hoping that we might be able to find constants  $a, b, c$  appropriate for each of several kinds of navigation or echo sounder technology. This attempt failed, for two reasons. First, the results sometimes did not converge to sensible values, due primarily to the presence of non-zero medians in the differences from each cruise. The Gulf Stream crosses our area and there is a large change in bulk sound velocity across this boundary current; if a cruise has a small error in sound velocity of the same sign over much of the depth range, then its data will be consistently shallower or deeper than the CCOTM grid. The second problem with the cruise-by-cruise approach is that we often couldn’t get enough metadata from the header files to make a sensible correlation of the parameters  $a, b, c$  with the ship’s navigation and bathymetric instruments.

By grouping the data into two bulk groups, one 1968 and older data, the other post-1968 data, we were able to get good fits. This somewhat arbitrary choice of groupings was motivated by the observation in Figure 10 that the older data had much larger errors, while the newer data had smaller errors. The values determined for parameters  $a, b, c$ , are shown in Table 1. The quantile-quantile plots for these two bulk aggregates of the data are shown in Figures 12a and 12b, where the

**Table 1** Error budget model parameters

	<i>a</i> (meters)	<i>b</i> (percent)	<i>c</i> (km)
Pre-1969	15	1.3	4.3
Post-1968	1	0.5	0.2

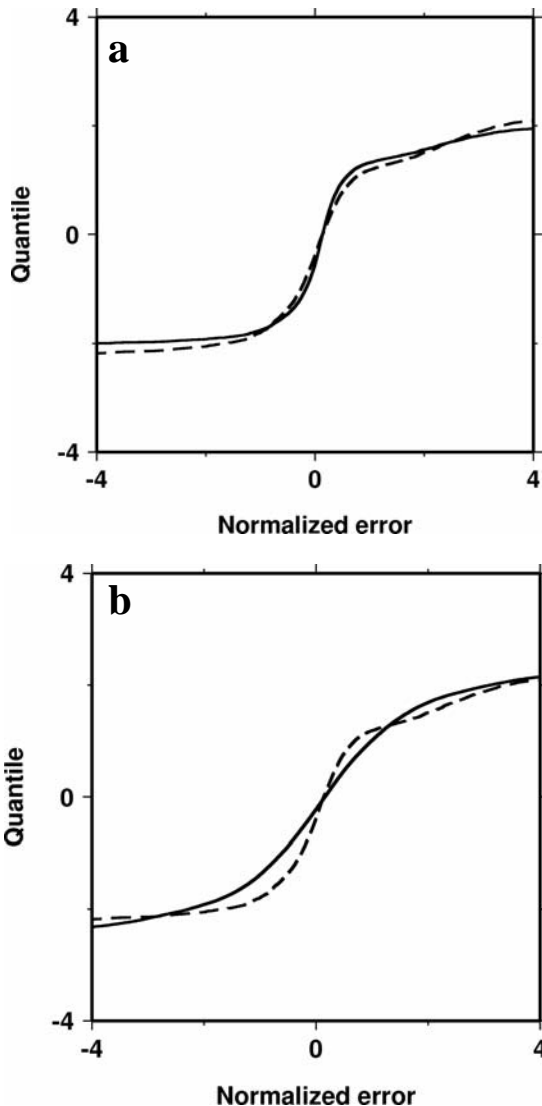


**Fig. 12** Q-Q plots of (a) pre-1969 errors, and (b) post-1968 errors. The departure of the curves from a one-to-one line indicates that errors larger than  $2\sigma$  are more common in these data than if they had ideal Gaussian (solid line) or Laplacian (dashed line) distributions

abscissa is  $e_i/\sigma$  using the table above, and the ordinate is a quantile, either Gaussian (solid lines) or Laplace (two-sided exponential). (Outliers are more likely in the Laplace distribution than in the Gaussian.) The flattening of the curves shows that errors larger than  $2\sigma$  are more common in these data than they should be if the errors had these ideal distributions.

This simple analysis of bulk aggregates of data

(shelf, slope and rise; smooth, flat areas and rugged canyons) with different potential sources of error spread across a range of depths from 15 to 5500 m. By aggregating different environments and instruments in one analysis we obtain an uncertainty estimate that depends solely on the reported depth, the age of the data, and the smoothed regional slope. This estimate can be made in the absence of detailed metadata about instrumentation and without prior knowledge of the geological environment surrounding the measurements. The smoothed regional slope may be estimated by smoothing a regional gridded model, such as those of Smith and Sandwell (1997). Thus our result, while doubtless an oversimplification, can be applied in the context of regional synthesis of heterogeneous data for deep water mapping, as was our goal.

### Conclusions

We developed an error budget by comparing single beam and multibeam echo sounder data in regions where they overlap. West of the Caroline Islands of Micronesia, well-navigated single beam tracks were subsequently covered by two or three multibeam swaths for up to 800 km of track line. The multibeam depths are repeatable to within 0.47% of depth (95% confidence), much smaller than the IHO S-44 Standard. The errors, which are manifest as an east-west tilt of the difference grids, are systematic and are consistent with roll bias in one or both swaths. We find that older single beam echo sounder data are as good as multibeam echo sounder data if we accept that the single beam system is averaging over the beam footprint, thus at wavelengths longer than about two beam footprints the two measurement technologies resolve the same seafloor features.

In the northwest Atlantic, we compare archival soundings made by various technologies to a recent multibeam grid. For post-1968 data, 95% of the errors (assuming the CCOM multibeam grid is “true”) are about what the IHO S-44 Standard expects, but the remaining 5% include some much larger errors, because the error distribution is non-Gaussian, contrary to the assumptions made in the IHO S-44 5<sup>th</sup> edition (IHO, 2008). The pre-1969 data errors are larger, with the 95<sup>th</sup> percentile error around five times worse. Most of the errors are attributable to navigational error and the largest are located in submarine canyons and at the edge of the shelf, where small navigation errors lead to large depth errors.

By fitting a standard deviation to best-fit a Gaussian quantile-quantile analysis over the middle 95% of the data, we determined a formula for the standard deviation of the expected error, assuming that error to be zero-mean. However, the data are not Gaussian and large errors occur in the last 5% of the data set; also, the

errors are not likely to be zero mean in any one cruise, due to sound velocity problems.

**Acknowledgements** This study was possible because the CCOM, JAMSTEC, and NGDC data sets were freely available for on-line download. We thank JAMSTEC (Contributors for MIRAI Data Web, (1999, 2000, 2001, 2002), MIRAI Data Web, <http://www.jamstec.go.jp/mirai/>, Japan Agency for Marine-Earth Science and Technology, Yokosuka, Japan) for making their multibeam echo sounder data freely available, the U.S. National Geophysical Data Center NGDC for making GEODAS, the Worldwide Marine Geophysical Database (<http://www.ngdc.noaa.gov/mgg/geodas/trackline.html>), freely available online, and the University of New Hampshire Center for Coastal and Ocean Mapping / NOAA Joint Hydrographic Center (CCOM) for making their surveys of potential extended continental shelf areas public. We thank two anonymous reviewers whose comments improved this manuscript. The views, opinions, and findings contained in this report are those of the authors and should not be construed as an official National Oceanic and Atmospheric Administration or U.S. Government position, policy, or decision.

This article is available online at:  
<http://www.springer.com/earth+sciences/oceanography/journal/11001>

## References

- Calder BR (2006) On the Uncertainty of Archive Hydrographic Datasets. *IEEE J Oceanic Eng* 31(2):249–265. doi:10.1109/JOE.2006.872215
- Carter DJT (1980) Echo-Sounding Correction Tables, 3<sup>rd</sup> edn. Hydrographic Department, Ministry of Defense, Taunton, United Kingdom
- Hare R (1995) Depth and position error budgets for multibeam echosounding. *Int Hydrogr Rev* LXXII(2):37-69
- International Hydrographic Organization (2008) IHO Standards for Hydrographic Surveys, 5<sup>th</sup> edn. Special Publication, 44, International Hydrographic Bureau, Monaco
- Jakobsson M, Calder B, Mayer L (2002) On the effect of random errors in gridded bathymetric compilations. *J Geophys Res.* 107(B12):2358. doi:10.1029/2001JB000616
- National Geophysical Data Center (2003) Worldwide Marine Geophysical Data, GEODAS Version 4.1.18 (CD-ROM). Boulder, Colorado, USA: Data Announcement 2003-MGG-02, US Department of Commerce, National Oceanic and Atmospheric Administration, Boulder, CO, USA
- Smith WHF (1993) On the accuracy of digital bathymetric data. *J Geophys Res* 98(B6):9591–9603. doi:10.1029/93JB00716
- Smith WHF (1998) Seafloor tectonic fabric from satellite altimetry. *Ann Rev Earth Planet Sci* 26:697-747. doi:10.1146/annurev.earth.26.1.697
- Smith WHF, Sandwell DT (1994) Bathymetric prediction from dense satellite altimetry and sparse shipboard bathymetry. *J Geophys Res* 99(B11):21803-21824. doi:10.1029/94JB00988
- Smith WHF, Sandwell DT (1997) Global sea floor topography from satellite altimetry and ship depth soundings. *Science* 277:1956-1962. doi:10.1126/science.277.5334.1956
- Wessel P, Smith WHF (1998) New, improved version of Generic Mapping Tools released. *EOS Trans AGU* 79:579. doi:10.1029/98EO00426